A Comparison of Linear Scaling Techniques for Analysis of Three-Dimensional Point Clouds

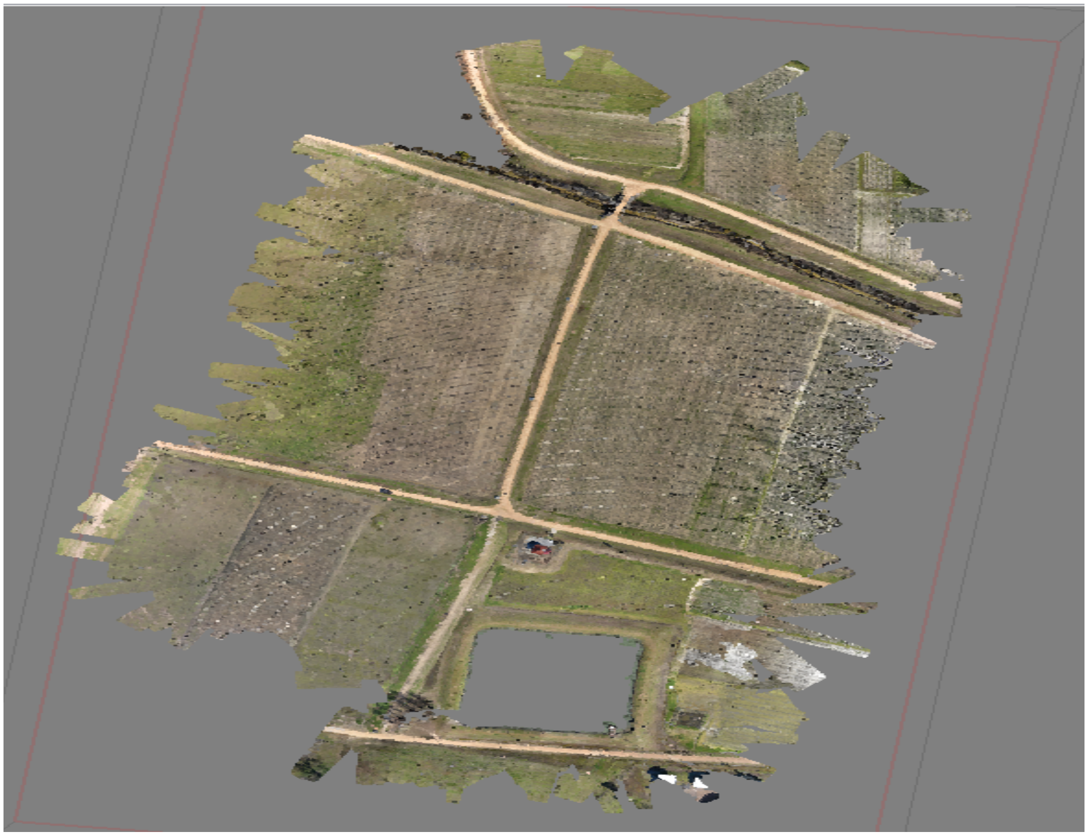

Abby Bassie, Gray Turnage, Sean Meacham, Lee Hathcock, and Robert J. Moorhead

Geosystems Research Institute, Mississippi State University, Mississippi State, MS 39762-9627

Geosystems Research Institute Report 5069

November 2016

A Comparison of Linear Scaling Techniques for Analysis of Three-Dimensional Point Clouds

Abby Bassie, Gray Turnage, Sean Meacham, Lee Hathcock, David Young, and Robert J. Moorhead

Geosystems Research Institute, Mississippi State University, Mississippi State, MS 39762-9627

Introduction

Unmanned air systems (UAS) are becoming an increasingly important platform for the acquisition of remote imagery in a wide variety of applications. In 2002, NASA may have pioneered UAS imagery collection for precision agriculture by conducting a proof-of-concept flight over a 1,500 ha plot owned by the Kauai Coffee Company in U.S. national airspace over Hawaii (Herwitz et al. 2004). During the flight, high-resolution color and multispectral imaging payloads were used to collect data. The images were geotagged with a GPS unit aboard the UAS and then used to map invasive weed locations within the field and detect irrigation and fertilization inconsistencies. This mission was key in proving the capability of UAS to locally monitor agricultural regions and to be a viable tool for precision agriculture.

Three-dimensional (3-D) reconstruction is one way that UAS imagery is used in precision agriculture. Red-Green-Blue (RGB) imagery is collected over a test plot and analyzed by 3-D reconstruction software. The software recognizes photographs of the same object taken from different angles and identifies the same object in multiple images; these are called conjugate pixels. Conjugate pixels are then stacked in a virtual 3-D space, and distances are estimated between the pixels to generate a point cloud. Point clouds are then scaled to represent the original surveyed area so the representative point cloud of the area can be dimensionally analyzed by linear measurement tools (LMT). These measurements can be used to quantitatively analyze test plots by determining size, shape, and location of items of interest in a test plot. This research analyzed two types of scaling techniques: user-defined and GPS-defined. User-defined scaling is established by the software user and is usually based upon measurements recorded with a measuring device at a field site. GPS-defined scales are based on GPS locations of objects and the calculated distance between them in the imagery collected. Scaling is critical to later use of LMT's, as the accuracy of the scale will affect all measurements subsequently calculated by LMT's. The purpose of this work was to compare the two scaling methods to determine accuracy of each when used in a field setting.

Materials and Methods

This report is a companion study to Bassie et al. (2016). Both reports used a Nikon RGB camera with a 10mm lens attached to a Precision Hawk Lancaster version 4 to capture imagery over an 8.86 ha (21.89 ac) test plot at the R.R. Foil Plant Research Center (North Farm) at Mississippi State University (Figure 1). Six flights were executed at 70% in track and side overlap between images. In-track overlap higher than 70% can cause triggering problems in the shutter system of the Nikon payload. The first flight was conducted at an altitude of 45.72 m (150 ft.), and subsequent flights were flown at increasing altitudes of 15.24 m (50 ft.) per flight. Nine predetermined reference objects (RO's, Figure 2) were geotagged with a handheld GPS unit (Trimble GEO-7X with centimeter accuracy) and measured with a measuring tape to the nearest centimeter prior to UAS flights to serve as points of reference for scaling and LMT's. Measurements of height (z), width (x), and length (y) were obtained from the RO's. Some RO's only had a few measurable dimensions, and other RO's had multiple measurable surface features (e.g. sewer caps, culvert caps, angular surfaces).

After obtaining imagery from each flight, the digital images from the flight plans were processed in AgiSoft PhotoScan (AgiSoft) to generate six point clouds (one per flight height). The dimensions of the nine RO's (Table 1) were used to determine the accuracy of linear measurements recorded by two software packages that utilize the different scaling techniques for generating point clouds, MeshLab and AgiSoft. The MeshLab LMT implements a user-defined scale in which the user must define the measurement of a known dimension of a RO within the point cloud. After establishing this point of reference, the rest of the point cloud is scaled accordingly. This method is discussed in detail in Bassie et al. (2016).

AgiSoft, however, utilizes a GPS-defined scale to establish the dimensions of objects within point clouds. During all flight scenarios, roll, pitch, yaw, latitude, longitude, and altitude were recorded for every image taken by the UAS. This data was then imported into AgiSoft to establish a GPS-defined scale for generated point clouds. After scaling the point clouds from each flight scenario, AgiSoft's LMT was used to dimensionally analyze the nine predetermined RO's. These measurements were then compared to the known dimensions of the RO's (See Appendix A). The difference in the LMT and predetermined values were recorded as Δx, Δy, and Δz. These values were then averaged at each altitude to determine mean change in each direction for the six flight scenarios (Table 2). Finally, comparisons were drawn between the scaling techniques as calibrators of LMT's for use in 3-D reconstructions generated from UAS captured imagery.

Results

The spatial resolution in the point clouds for all six flight scenarios was too low to clearly differentiate between the angular surfaces atop RO's five and nine, so these were not used in the analysis of AgiSoft's LMT. When MeshLab was used to perform linear measurements on the six point clouds generated by the image dataset, there was a substantial loss of point cloud resolution at high flight altitudes. Only two measurements could be made on the point cloud generated from images captured at 121.92 m (400 ft.) in MeshLab (Bassie et al. 2016). When AgiSoft's LMT was used to make dimensional measurements on the point clouds, the correlation between loss of point cloud resolution and flight altitude was much less prevalent. AgiSoft point clouds had enough spatial resolution to make a total of 10 dimensional measurements on the RO's both on the lowest (45.72 m) and highest flight altitudes (121.92 m, Appendix A). Since point clouds generated by AgiSoft are directly imported into MeshLab for analysis, clouds from a given flight scenario should theoretically have the same resolution whether they are viewed in MeshLab or AgiSoft. The observation of decreased point cloud resolution in MeshLab could suggest a loss of point density upon point cloud import into MeshLab.

When AgiSoft was used to analyze the six point clouds, average Δx, Δy, and Δz values were obtained for all flight scenarios. MeshLab, on the other hand, was unable to make any measurements in the 'y' direction at 121.92 m (400 ft.) and was unable to make measurements in any direction on the point clouds at 45.72 (150 ft.) and 60.96 m (200 ft.) because the large image count at those altitudes caused the software to crash (Bassie et al. 2016). In comparison to the user-defined scale LMT, the GPS-defined scale yielded smaller Δx, Δy, and Δz values in 83.33% of the flight scenarios (Table 2).

Discussion and Conclusions

The results of this study suggest that establishing scale with a GPS-defined method yields more accurate point clouds than a user-defined scale. While the performance of MeshLab's LMT on the dataset suggested that the lower the altitude, the higher the spatial resolution of point clouds (Bassie et al. 2016), AgiSoft's performance on datasets seems to be less affected by the altitude at which imagery is collected. This contrast could be caused by the different scaling methods implemented within the two software packages. When imagery is collected from high flight altitudes, point clouds can lose a significant amount of point density, causing object edges to become less apparent. This reduced point cloud resolution decreases the accuracy of a user-defined scale, as object edges must be used to set the scale of the point cloud. While altitude changes very likely affect the accuracy of a user-defined scale, a GPS-defined scale is less vulnerable to error since GPS data is fixed in space and is generally not affected by small changes in flight altitude. Still, in both scaling methods, user error will usually occur when measuring a scaled point cloud with a LMT since the user must determine the edges of objects to be measured within point clouds; the extent of this error will be affected by point cloud density and user precision in both user-defined and GPS-defined point clouds.

In every flight scenario conducted in this study, linear measurements in x, y, and z directions deviated from actual measurements by less than 10% when using a GPS-defined scale. In comparison, measurements based on a user-defined scale deviated from actual measurements by less than 10% in the x, y, and z directions in only three of the six flight scenarios (Bassie et al. 2016). This observation was expected, as scaling point clouds manually can introduce a degree of user error that decreases the accuracy of linear measurements.

The results of this study suggest that a GPS-defined scaling method yields the most accurately scaled point clouds of a test area. A computer algorithm to "assist" in the detection of object edges would likely improve the accuracy of linear measurements of objects within a GPS-defined point cloud. This type of algorithm could help eliminate a large portion of the user error that is inevitably introduced when a user manually selects the endpoints of a distance to be measured. This algorithm could be especially useful in high altitude flights with low point density for ground objects. In this type of scenario, an algorithm to detect object edges could be used in tandem with a user's defined points of interest to determine a best-fit distance between the identified object edges. A software package with this capability could be an indispensable tool for analyzing objects within a three-dimensional point cloud.

Literature Cited

Bassie, A., S. Meacham, D. Young, G. Turnage, and R. J. Moorhead. 2016. 3D Reconstruction Optimization Using Imagery Captured by Unmanned Aerial Vehicles. GRI Technical Report #5068. Mississippi State University: Geosystems Research Institute. 10p.

Herwitz, S.R., L.F. Johnson, S.E. Dunagan, R.G. Higgins, D.V. Sullivan, J. Zheng, B.M. Lobitz, J.G. Leung, B.A. Gallmeyer, M. Aoyagi, R.E. Slye, and J.A. Brass. 2004. Imaging from an unmanned aerial vehicle: agricultural surveillance and decision support. *Computers and Electronics in Agriculture* 44(1): 49-61.

Tables and Figures

Table 1. Reference objects and their actual dimensions**

Reference Object #	x (cm)	y (cm)	z (cm)
1	149.86	149.86	69.85
2a	78.74	-	54.61
2b	66.04	-	-
2c	98.1	-	-
3a	147.32	-	-
3b	64.77	-	16.71
4a	98.11	-	-
4b	78.74	-	-
5	-	-	-
6	66.04	66.04	-
7	97.16	78.74	80.01
8a	78.74	98.11	-
8b	98.11	-	-
9	-	-	38.10

*Total width of R.O. #8 x (cm) = 98.1075

**Multiple dimensions on the same RO are listed as a, b, c, etc.

Table 2. Average change from actual measurements for each flight scenario.

Altitude (m)	Δx (cm)	Δy (cm)	Δz (cm)	Area (Ha)	Image Count
400	0.05	-4.060	**3.30**	8.86	156
350	3.07	-1.524	-6.668	8.86	190
300	0.054	**6.858**	**3.048**	8.86	225
250	-2.223	-6.710	-0.254	8.86	360
200	0.733	1.956	7.239	8.86	533
150	4.434	2.942	-5.842	8.86	927

*values shown in bold deviated less from the actual measurement when MeshLab's linear measurement tool was used (Bassie et al. 2016).

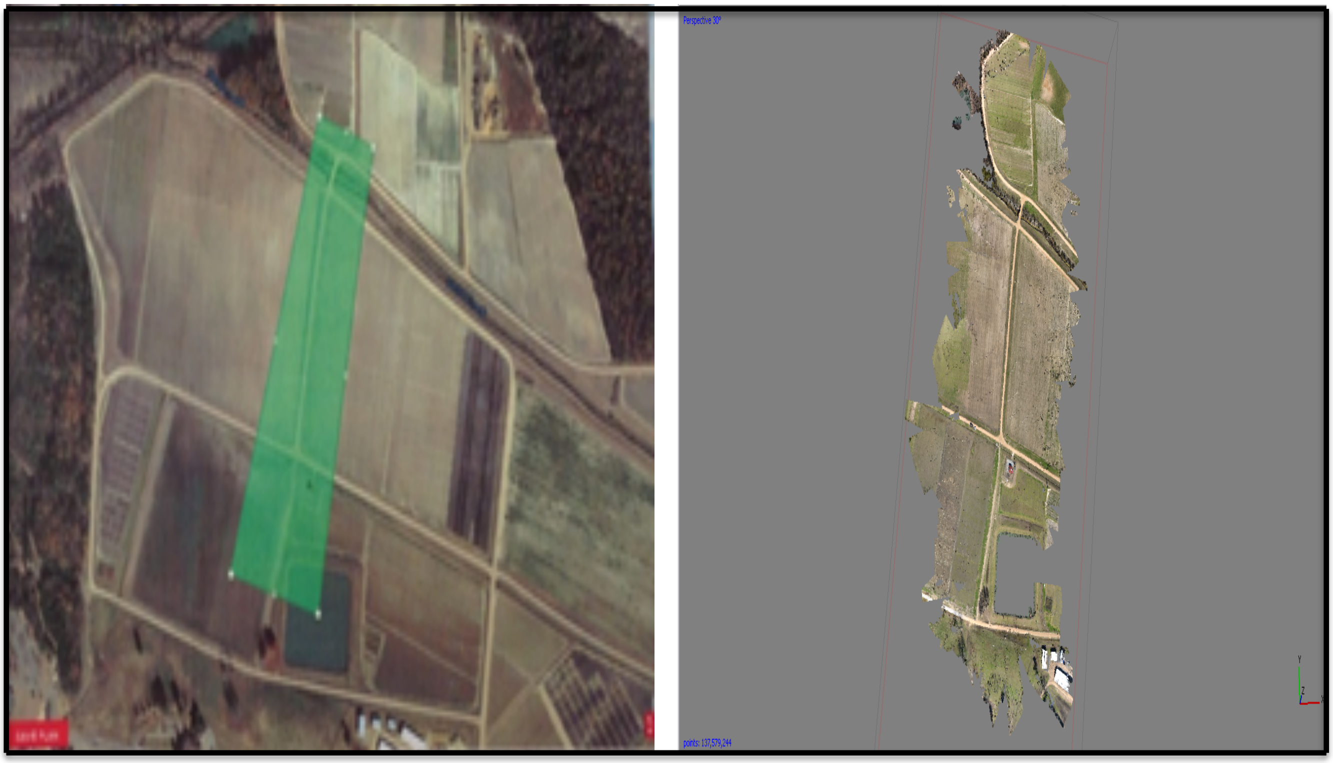

Figure 1. Flight plan over the R.R. Foil Plant Research Center at Mississippi State University (left) and imagery collected over the same site (right).

Figure 2. Reference objects at the R .R. Foil Plant Research Center at Mississippi State University.

Appendices

Appendix A. The deviation of AgiSoft measurements from actual measurements of reference object dimensions. Values are shown (+) when AgiSoft measurements were larger than the actual measurement and (-) when AgiSoft measurements were less than the actual measurements. All values are given in cm. Any measurements that could not be performed in AgiSoft are marked with
"-- --".

Reference Object #	Dimension	150	200	250	300	350	400
1	ΔX	+5.080	-1.854	-2.413	+2.54	-3.048	+2.286
	ΔY	-1.778	+0.864	-- --	-- --	+0.762	-- --
	ΔZ	-5.842	-- --	-1.778	+3.048	+8.128	-- --
2	ΔX	+3.302	4.826	+1.270	+2.286	-6.858	+5.017
	ΔY	-- --	-- --	-- --	-- --	-- --	-- --
	ΔZ	-- --	-- --	+1.270	-- --	-- --	+3.302
3	ΔX	-5.588	-1.270	+2.286	-1.651	+3.556	-3.048
	ΔY	-- --	-- --	-5.080	-- --	-- --	-- --
	ΔZ	-- --	-- --	-- --	-- --	-- --	-- --
4	ΔX	-1.080	-2.286	-1.100	-- --	-6.668	-7.620
	ΔY	-- --	-- --	-- --	+3.048	-- --	-- --
	ΔZ	-- --	-- --	-- --	-- --	-- --	-- --
5	ΔX	-- --	-- --	-- --	-- --	-- --	-- --
	ΔY	-- --	-- --	-- --	-- --	-- --	-- --
	ΔZ	-- --	-- --	-- --	-- --	-- --	-- --
6	ΔX	-- --	-- --	-- --	-- --	-- --	-- --
	ΔY	-5.080	+3.048	-3.048	+2.700	+2.032	+4.064
	ΔZ	-- --	-- --	-- --	-- --	-- --	-- --
7	ΔX	-5.969	+7.239	-9.271	-- --	+8.763	-1.143
	ΔY	-- --	-0.254	-- --	-2.450	-- --	-- --
	ΔZ	-- --	-- --	-- --	-- --	-- --	-- --
8	ΔX	+1.969	-- --	-- --	-- --	-- --	+12.891
	ΔY	-- --	-- --	-12.00	-- --	-- --	-- --
	ΔZ	-- --	-- --	-- --	-- --	-- --	-- --
9	ΔX	-- --	-- --	-- --	-- --	-- --	-- --
	ΔY	-- --	-- --	-- --	-- --	-- --	-- --
	ΔZ	-- --	-- --	-- --	-- --	-- --	-- --